Amygdala engages non-emotional multi-item working memory maintenance through amygdala-hippocampus interaction

Chenyang Li[1], Yulong Peng[1], Ruixue Wang[2], Xianhui He[3], Ying Cai[3], Yuehui Ma[4], Dengchang Wu[5]*, Minmin Wang[6]* and Shaomin Zhang[7]*

[1]Qiushi Academy for Advanced Studies, Department of Biomedical Engineering, Zhejiang University, Hangzhou, 310027, China.
[2]Department of Neurosurgery, Third Affiliated Hospital of Naval Medical University, Shanghai, 200438, China.
[3]Department of Psychology and Behavioral Sciences, Zhejiang University, Hangzhou, 310058, China.
[4]Department of Neurosurgery, The First Affiliated Hospital, School of Medicine, Zhejiang University, Hangzhou, 310003, China.
[5]Department of Neurology, The First Affiliated Hospital, School of Medicine, Zhejiang University, Hangzhou, 310003, China.
E-mail: wudengchang@zju.edu.cn
[6]Westlake Institute for Optoelectronics, Westlake University, Hangzhou, 310007, China.
E-mail: minminwang@zju.edu.cn
[7]Qiushi Academy for Advanced Studies, Key Laboratory of Biomedical Engineering of Ministry of Education, Zhejiang Provincial Key Laboratory of Cardio-Cerebral Vascular Detection Technology and Medicinal Effectiveness Appraisal, Zhejiang University, Hangzhou, 310027, China.
E-mail: shaomin@zju.edu.cn

Keywords: working memory, maintenance, amygdala, amygdala-hippocampus interaction, intracranial EEG

Abstract

The process of holding information in working memory (WM) is an active one that requires neural activity within and between regions. The human amygdala (AMY) and hippocampus (HPC) are known to play crucial roles in emotional WM processing. Although human electrophysiological studies have made remarkable progress in revealing that HPC supports multi-item maintenance in a load-dependent manner, the characteristics of AMY and the circuit-level mechanisms underpinning AMY-HPC interactions remain largely unexplored. To address this gap in our knowledge, this study employed intracranial EEG recordings from AMY and HPC in nine epileptic patients to evaluate intra-regional neural representations and inter-regional communications during maintenance under different non-emotional WM loads. The results showed that high load enhances low-frequency power and intra-regional theta-gamma phase-amplitude coupling (PAC) in AMY and HPC. On the network level, high load elicits an increase in the strength of the modulation of HPC theta phase entraining AMY gamma amplitude. Furthermore, high load elevates AMY-aHPC theta phase synchrony and directional connectivity strength, with the direction being from anterior HPC (aHPC) to AMY. Conversely, posterior HPC (pHPC)-AMY synchrony is not affected by load variations. Overall, these findings highlight the importance of AMY in non-emotional WM tasks and shed new light on the neurophysiological basis of AMY-HPC interactions during WM maintenance.

1. Introduction

Working memory (WM), the capability of maintaining and manipulating information over a short period of time,[1] is crucial for higher-level cognitive functions.[2] WM tasks comprise encoding, maintenance, and retrieval phases, with the maintenance phase serving as a central component as it distinguishes WM from other types of memory.[3,4] Maintenance is pivotal for successful WM performance, as it requires keeping neural representations active even in the absence of external stimuli.[5] The amount of information to be kept in mind, i.e., WM load, has been shown to affect neural processing.[6] Exploring the effects of WM load can enhance our understanding of how the brain coordinates different regions to accomplish complex cognitive tasks. In humans, the amygdala (AMY) and hippocampus (HPC) are thought to be involved in WM processing.[7–9] Although electrophysiological studies in humans have shown that HPC supports non-emotional multi-item maintenance in a load-dependent manner, the role of AMY

and AMY-HPC interactions in supporting non-emotional WM maintenance and their cognitive load-dependent properties remain largely unexplored.

Recent studies have indicated that HPC is a critical region involved in WM maintenance, especially when dealing with an increasing cognitive load.[10–13] While AMY has traditionally been thought to be related only to emotions, recent findings indicate that it also participates in non-emotional WM memory. The multi-dimensional response characteristics of this region, such as blood oxygen level-dependent (BOLD) responses and sustained neural activity are found to be dependent on memory loads.[14,15] In addition, activation of AMY via electrical stimulation or peripheral drug administration could enhance non-emotional memory consolidation.[16–19] These existing studies suggest that AMY activity is critical for modulating memory in the absence of emotional stimuli. Evidence for AMY involvement in WM maintenance was provided by the fact that the degree of phase locking of AMY selective neurons is load-dependent, with increased phase locking in higher loads.[20] While another study failed to provide evidence supporting AMY involvement in maintenance, this was attributed to the inability of AMY neuronal activity to decode load levels during WM maintenance.[21] Hence, whether AMY is involved in WM maintenance and shows load dependency is under intensive debate.

WM relies on coordinated processing between functionally interconnected brain regions.[22] The interactions between AMY and HPC have been extensively proposed to support emotional memory processes.[23–25] Recent evidence suggests that AMY-HPC interactions are pivotal to non-emotional WM tasks, and it has been shown that memory load can be decoded by the information flow from HPC to AMY in the low-frequency band during maintenance.[26] Notably, HPC is not a unitary structure and the interconnections between AMY and HPC subregions are complex.[27] HPC can be divided into anterior and posterior parts (aHPC and pHPC), corresponding to the ventral and dorsal HPC in rodents, which exhibit differences in function, structure, and connections to cortical and subcortical areas.[28,29] For example, selective inactivation of ventral but not dorsal glutamatergic HPC neurons suppressed the synaptic consolidation of memory.[30] Currently, the evidence supporting the involvement of human AMY-HPC circuits in WM is insufficient. Furthermore, it remains unclear whether the connectivity between AMY and distinct HPC subregions exhibits different patterns during WM maintenance. Intracranial electroencephalography (iEEG) provides a novel technique that allows for simultaneous measurements from multiple specific recording sites of interest.[2]

To investigate the role of AMY and AMY-HPC interactions during WM maintenance, we analyzed iEEG recordings from AMY and HPC (including both aHPC and pHPC) in nine epileptic patients.[31] A modified Sternberg paradigm was implemented, and the patients performed a verbal WM task that included trials of different set sizes. WM load was determined by the number of letters. Our results showed enhanced low-frequency power and intra-regional theta-gamma phase ampitude coupling (PAC) under the high load condition in both AMY and HPC during maintenance. On the network level, high WM load elicited an increase in the modulation strength of HPC (including both aHPC and pHPC) theta phase entraining AMY gamma amplitude. Addtionally, aHPC and pHPC exhibited divergent connectivity patterns with AMY, which was characterized by increased AMY-aHPC theta phase synchrony and directional connectivity strength under the high-load condition, with the influence direction being from aHPC to AMY, while pHPC-AMY theta phase synchrony was not affected by memory load. These above load-dependent connectivity characteristics significantly contribute to behavioral success. Taken together, our study underscores the importance of AMY in non-emotional memory tasks and provides a novel insight into the neurophysiological basis of human AMY activity and AMY-HPC interaction during WM maintenance.

2. Results

2.1. Task, behavior and electrode locations

Nine epilepsy patients (5 females and 4 males) participated in a modified Sternberg WM task (**Figure 1A**), totaling 37 sessions across all subjects (see Experimental Section for details). All subjects performed well on the task with the correct response rate 92.3 ± 2.7% (both for IN and OUT trials across set size 4, 6 and 8). As illustrated in the original work, the mean memory capacity was identified as 6.8 in this dataset,[31] reflecting the limited number of objects that could be held in the WM. Given that the inter-regional coupling pattern varied between conditions below and above the capacity limit,[32] in our study, the low and high WM load refers to trials with set size 4 and 6, both of which were under the capacity limit. The subjects achieved higher accuracy under the low-load condition (98.7 ± 1.6% correct responses) as compared to the high-load condition (91.3 ± 4.4% correct responses) ($t(8) = 5.717$, $p = 0.0004$, paired t-test). Across all subjects, the response time (RT) for correct trials significantly increased with WM load from set size 4 to 6 (1.2 ± 0.2 s versus 1.4 ± 0.2 s, respectively) ($t(8) = 4.664$, $p = 0.0016$,

paired t-test) (**Figure 1B**). Both behavioral measures (accuracy, RT) were load-dependent, exhibiting better performance under the low-load condition.

Across 9 patients, we analyzed iEEG data from a total of 30, 32, and 32 electrodes in AMY, aHPC, and pHPC, respectively (**Figure 1C**). All analyses in this study were conducted after bipolar-referenced processing. Across all subjects, the number of electrode pairs covering AMY-aHPC within the same hemisphere was 60, and the count for AMY-pHPC was 56.

Figure 1. Task, behavior and electrode locations. A) Experimental paradigm. B) Behavioral results included accuracy (percentage correct, %) and RT (s) for the correct trials. Dots indicate individual results. ***p<0.001, **p<0.01. C) Selected electrodes localizations across 9 subjects in the MNI space.

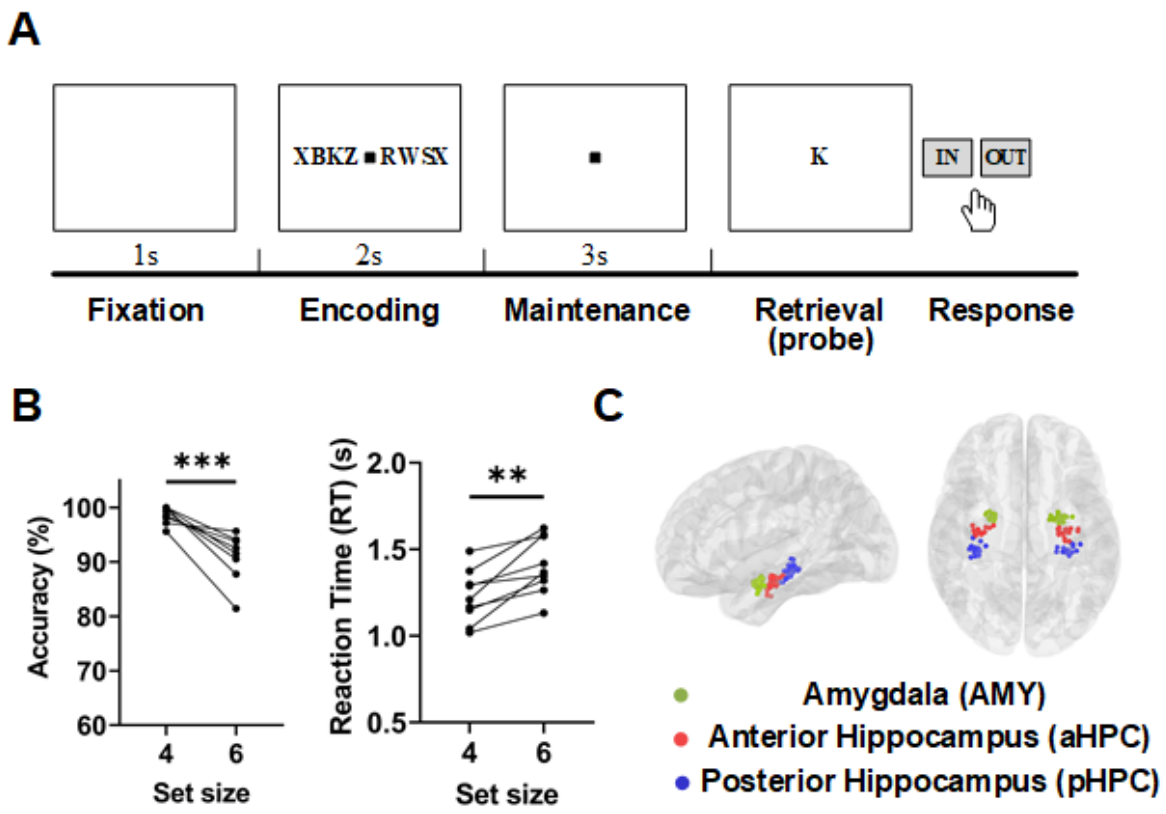

2.2. Load-dependent low-frequency power in AMY during WM maintenance

To investigate the influence of WM load on the activities of AMY during maintenance, we analyzed the low-frequency (3–8 Hz theta range and 8–13 Hz alpha range) power responses of AMY for the correct trials under the low- and high-load conditions. The time-frequency results

indicated significant load effects on clusters in AMY, as well as in aHPC and pHPC, with a notable increase in low-frequency power for the high-load condition (cluster-based permutation, $p < 0.05$, **Figure 2A**).

We subsequently extracted and averaged the power within the theta and alpha band in AMY, aHPC and pHPC, and then compared these powers between the low- and high-load conditions during WM maintenance. We found that the high loads resulted in increased theta and alpha powers (**Figure 2B**) in all three brain regions (aHPC, theta: $p = 0.0006$; alpha: $p = 0.0012$; pHPC, theta: $p = 0.0358$; alpha: $p = 0.0013$; AMY, theta: $p = 0.0003$; alpha: $p = 0.0028$; Wilcoxon signed-rank test). The increased low-frequency power of HPC under the high-load condition was consistent with previous studies.[11,12]

To validate that the observed power changes were induced by the WM tasks, we compared the powers during the WM maintenance period with those of the baseline (zero) and found an increase in low-frequency power in AMY, aHPC and pHPC (**Figure 2B**), especially under the high-load condition. Specifically, AMY and aHPC exhibited task-induced power increases in the theta band under the low- and high-load conditions (AMY low load: $p = 0.0011$, high load: $p < 0.0001$; aHPC low load: $p = 0.0093$, high load: $p < 0.0001$; one sample Wilcoxon test), while significant power changes in pHPC were observed only under the high-load condition (low load: $p = 0.1966$; high load: $p = 0.0088$; one sample Wilcoxon test). In the alpha band, only aHPC displayed a significant power increase under both load conditions (low load: $p = 0.0454$; high load: $p < 0.0001$; one sample Wilcoxon test). The significant increase of alpha power in AMY was observed exclusively under the high-load condition (low load: $p = 0.1772$; high load: $p = 0.0035$; one sample Wilcoxon test), whereas no task-induced power changes in pHPC were found under either load condition (low load: $p = 0.7053$; high load: $p = 0.0521$; one sample Wilcoxon test). Taken together, these results may suggest that not only HPC (including aHPC and pHPC) is involved in maintenance and exhibits load-dependency, but also AMY is recruited, with its activity being affected by WM load in a manner similar to HPC. Notably, these three regions exhibited load dependency within different temporal ranges on the time-frequency spectrum, suggesting that they may have distinct roles in WM maintenance.

Figure 2. Theta and alpha power in AMY, aHPC and pHPC during maintenance for the correct trials. A) Low-frequency time-frequency representation of spectral power. Time '0' indicates the onset of the retrieval period. B) Extracted and averaged theta (3–8 Hz) and alpha

(8–13 Hz) power for low- and high-load trials. Errors bars represent standard errors of the mean (SEM) across all selected electrodes. Symbols represent statistically significant difference: * compared to different load; # compared to baseline. ***p<0.001, **p<0.01, *p<0.05; ####p<0.0001, ##p<0.01, #p<0.05.

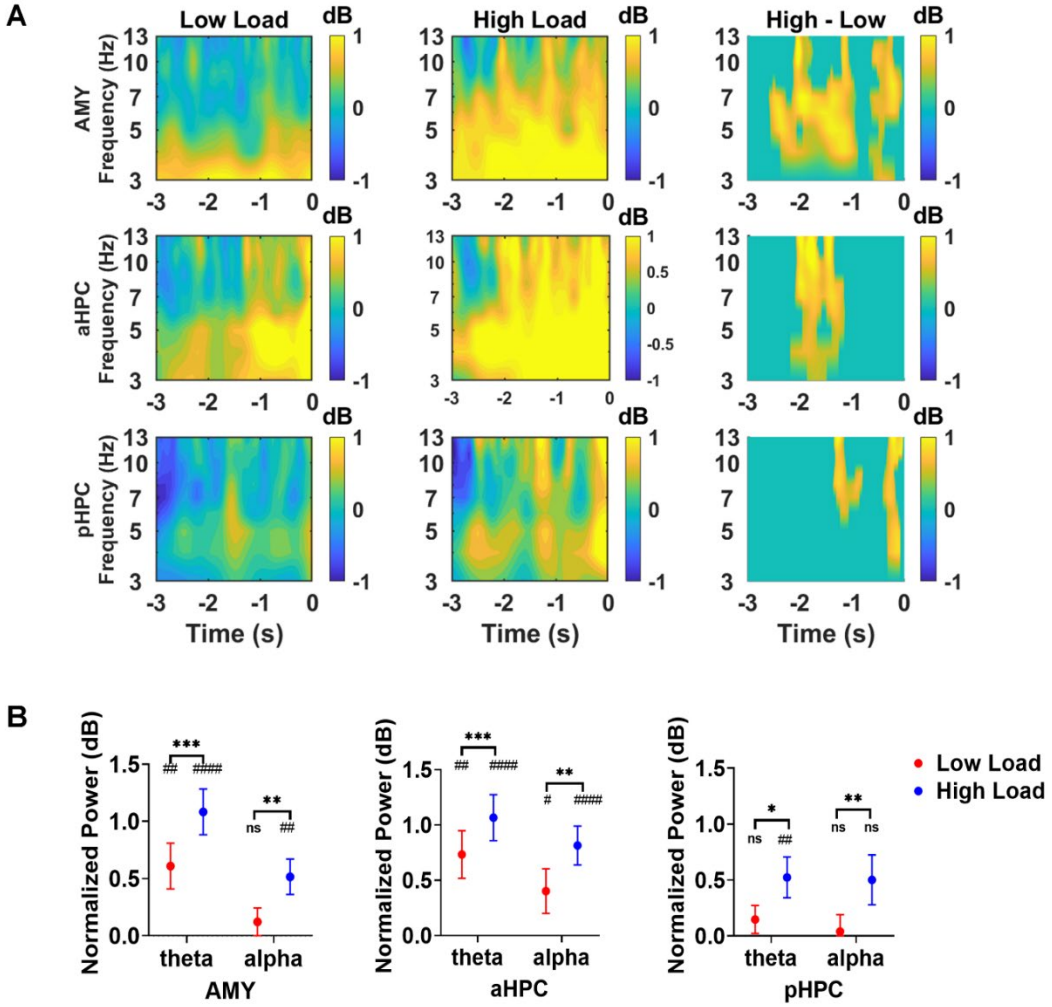

2.3. Greater theta-gamma phase-amplitude coupling in AMY under the high-load condition during WM maintenance

It has been suggested that the organization of WM for multiple items is facilitated by theta-gamma coupling in HPC during maintenance.[10,33,34] One may wonder whether the neural mechanism of theta-gamma coupling in AMY could coordinate WM maintenance. To check for this potential modulation, we calculated theta-gamma PAC values for the correct trials during maintenance under different load conditions. Then, the raw PAC was z-scored against null distribution. The results showed that the theta phase entrained the gamma amplitude in AMY (low-load condition: peak at 7 Hz and 73 Hz for phase and amplitude frequencies; high-

load condition: peak at 8 Hz and 78 Hz for phase and amplitude frequencies; **Figure 3A** left), aHPC (low-load condition: peak at 7 Hz and 98 Hz for phase and amplitude frequencies; high-load condition: peak at 5 Hz and 93 Hz for phase and amplitude frequencies; **Figure 3A** middle) and pHPC (low-load condition: peak at 5 Hz and 98 Hz for phase and amplitude frequencies; high-load condition: peak at 4 Hz and 98 Hz for phase and amplitude frequencies; **Figure 3A** right). Notably, the peak PAC value of AMY was located at a higher phase frequency and a lower amplitude frequency compared to both aHPC and pHPC, suggesting that the load-dependent PAC in AMY may not be attributed to volume conduction.

As a first step, we assessed for task-induced changes in the strength of intra-regional PAC during maintenance over baseline. Across all loads, we found that the pattern of the intra-regional PACs in three brain areas during maintenance were increased relative to the baseline (all $p < 0.0001$; Wilcoxon signed-rank test) (**Figure 3B**). To compare the intra-regional PAC between different load conditions, we extracted and averaged the normalized theta (3–8 Hz) - gamma (30–100 Hz) PAC value for each effective electrode. We observed that AMY exhibited a significant enhancement in theta-gamma PAC under the high-load condition compared to the low-load condition ($p = 0.048$, Wilcoxon signed-rank test). Similar to previous study,[10] our results also showed that simultaneous maintenance of multiple items in WM is accompanied by theta-gamma coupling in HPC. We found significantly higher values of intra-regional theta-gamma PAC under the high-load condition for both aHPC and pHPC (aHPC: $p = 0.0015$; pHPC: $p = 0.0473$; Wilcoxon signed-rank test) (**Figure 3B**). Taken together, our results confirmed the engagement of AMY in the maintenance process and demonstrated that WM load enhanced the inter-regional theta-gamma PAC not only for aHPC and pHPC but also for AMY.

Figure 3. Intra-regional theta-gamma PAC in AMY, aHPC and pHPC for the correct trials. A) Averaged phase-amplitude comodugram during maintenance. Warmer colors indicate stronger modulation; B) Averaged the theta (3–8 Hz)- gamma (30–100 Hz) PAC during baseline, low-load and high-load maintenance. Error bars represent the SEM. ****$p<0.0001$, **$p<0.01$, *$p<0.05$.

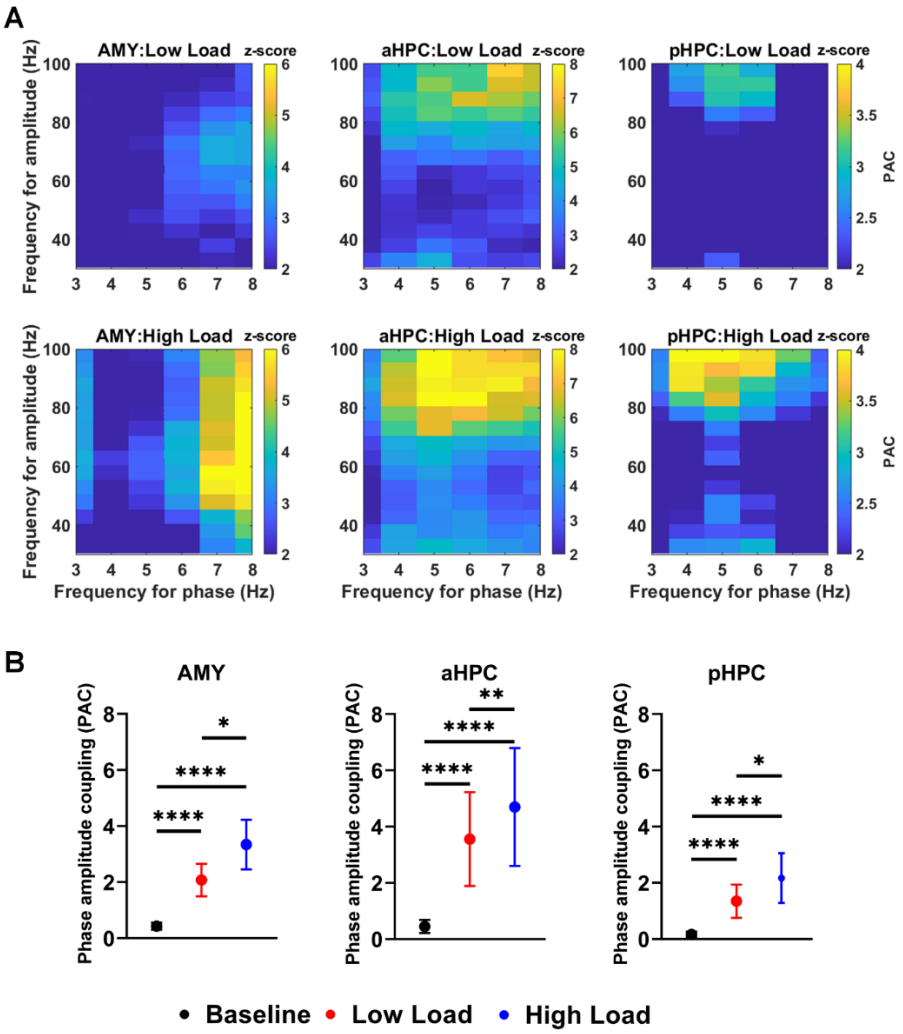

2.4. Load-dependent AMY-aHPC theta synchrony during WM maintenance

Considering the supposed role of low-frequency oscillations in inter-regional communication,[35] and the putative function of theta rhythm in coordinating AMY and HPC systems,[36] we investigated the phase synchrony between AMY and HPC of the correct trials during maintenance under different load conditions. The weighted Phase Lag Index (wPLI) serves as a conservative measure of phase synchrony, offering the advantages of low sensitivity to the volume conduction and uncorrelated noise sources.[37] The connectivity measure wPLI was computed over AMY-aHPC and AMY-pHPC, respectively. This analysis was performed with the significant electrode pairs (see Experimental Section for details), including 48 pairs for AMY-aHPC and 33 pairs for AMY-pHPC, respectively.

As shown in **Figure 4A**, the time-frequency domain wPLI revealed the dynamic fluctuations of phase synchrony between each two regions in specific frequency ranges during maintenance.

We first tested whether maintenance periods showing task-induced phase synchrony for both AMY-aHPC and AMY-pHPC circuits under different load conditions. We quantitatively averaged the theta band wPLI from 3 to 8 Hz and found that the phase synchrony during maintenance exhibited significant task-induced enhancement under the high-load condition for both AMY-aHPC and AMY-pHPC ($p = 0.0007$ and $p < 0.0001$ for AMY-aHPC and AMY-pHPC; Wilcoxon signed rank test, **Figure 4B**). However, theta phase synchrony between AMY and aHPC was not significantly higher for maintenance versus baseline under the low-load condition, while AMY-pHPC showed task-induced theta phase synchrony ($p = 0.2427$ and $p = 0.0022$ for AMY-aHPC and AMY-pHPC; Wilcoxon signed rank test, **Figure 4B**). Next, we explored the effect of WM load on theta phase synchrony during maintenance for both AMY-aHPC and AMY-pHPC. The results showed significant load effect in AMY-aHPC with an increase of wPLI for the high-load condition relative to the low-load condition ($p = 0.0053$, Wilcoxon signed rank test; **Figure 4B**). However, no significant difference in theta band wPLI of AMY-pHPC under different load-conditions was found ($p = 0.1827$, Wilcoxon signed rank test, **Figure 4B**). These results suggest that there might be differences in the responses of aHPC and pHPC to WM load. Additionally, we also evaluated the phase synchrony in the alpha band (from 8 to 13 Hz) between AMY and two HPC subregions. We found that there was no significant difference between the baseline and maintenance for both AMY-aHPC (baseline vs. low-load maintenance: $p = 0.9070$, baseline vs. high-load maintenance: $p = 0.1963$; Wilcoxon signed rank test) and AMY-pHPC (baseline vs. low-load maintenance: $p = 0.3483$, baseline vs. high-load maintenance: $p = 0.5135$; Wilcoxon signed rank test) in the alpha band, regardless of the load condition (**Figure 4C**). Although we observed alpha phase synchrony between AMY and pHPC was not significantly higher during maintenance versus baseline, high load in WM resulted in higher AMY-pHPC alpha phase synchrony ($p = 0.0443$, Wilcoxon signed rank test) (**Figure 4C**). By contrast, phase synchrony between AMY and aHPC showed no difference in the alpha band between low- and high-load conditions. Together, these results show clear evidence that multi-item WM maintenance is associated with increased theta phase synchrony between AMY and HPC. Moreover, we found that WM load had divergent effects on the connectivity patterns between AMY and HPC subregions.

Figure 4. Inter-regional phase synchrony over AMY-aHPC and AMY-pHPC for the correct trials. A) Phase synchrony (i.e., wPLI) under the low- and high-load conditions. The wPLI value ranges from 0 to 1, with warmer colors indicating greater phase synchrony. Time '0' indicates the onset of the retrieval period. B) and C) Extracted theta and alpha wPLI during baseline,

low- and high-load maintenance. Error bars indicate the SEM across electrode pairs. ****p<0.0001, ***p<0.001, **p<0.01, *p<0.01.

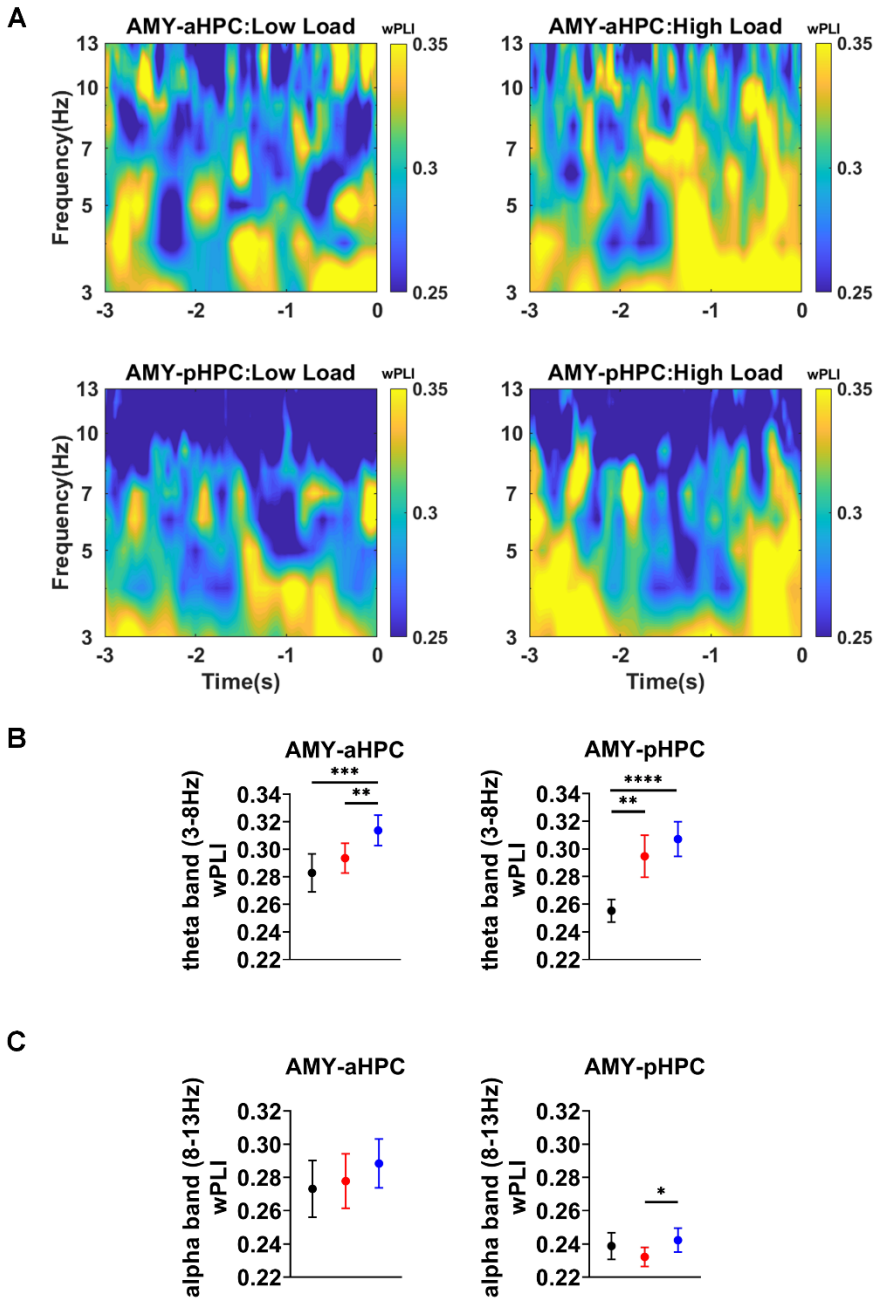

2.5. WM load effects on directional interaction of between AMY and HPC in the theta band

To elucidate the directionality of information transfer between different brain areas, we utilized frequency-domain Granger causality (GC) analysis in addition to wPLI measurements, which only reveal non-directional interactions. The GC analysis assesses the extent to which the

incorporating information from one region improves the predictability of the signal from the other region. Specifically, we investigated the directionality of information transfer over AMY-aHPC and AMY-pHPC circuits for the correct trials within the theta band (3–8 Hz), and also explored how the strength of effective connectivity varied with different load conditions during maintenance.

Firstly, we computed the GC index in the theta band for aHPC-AMY and pHPC-AMY. Only in the aHPC-to-AMY direction, a significantly stronger GC was observed under the high-load condition compared to the low-load condition (**Figure 5A**; $p = 0.008$, Wilcoxon signed rank test). Then, we estimated the directionality of net information flow over aHPC-AMY and pHPC-AMY. The results of net information flow ΔGranger (GC index of aHPC-to-AMY minus GC index of AMY-to-aHPC) revealed that the directional influence in the theta band from aHPC to AMY was significantly greater under the high-load condition (**Figure 5B**; $p = 0.0423$, Wilcoxon signed rank test); while there was no significant directional preference between AMY and pHPC. Taken together, our findings indicated that the theta-driven directional influence from aHPC to AMY was highly load-dependent, exhibiting increased causal connectivity under the high-load condition compared to the low-load condition. This observation aligns with the phase synchrony results, indicating that the WM load regulates the connectivity strength between AMY and aHPC.

Additionally, we re-assessed the information flow direction in the theta band between AMY and aHPC/pHPC under different load conditions by employing a phase slope index (PSI), which is more insensitive to mixtures of independent sources than GC.[38] We found that the load-dependent directional influence was specific to aHPC-AMY circuit, characterized by significantly stronger unidirectional aHPC-driven connectivity under the high-load condition (high vs. low: mean z-scored PSI 2.3687 vs. 1.4547, $p = 0.0092$, Wilcoxon signed rank test) (**Figure 5C** left). However, no significant directional influence within the pHPC-AMY circuit was observed between low- and high-load trials (**Figure 5C** right). This result was consistent with the results from the GC analysis that aHPC-AMY theta phase synchrony was load-dependent, with high load eliciting stronger directional connectivity from aHPC to AMY.

Figure 5. Directional information flow in the theta band of AMY-aHPC and AMY-pHPC during maintenance under different load conditions for the correct trials. A) GC index. B) Net information flow (ΔGranger). C) Z-scored PSI value. Positive values indicate that aHPC (left)

or pHPC (right) leads AMY, negative values indicated that AMY leads aHPC or pHPC. Error bars represent the SEM. **p<0.01, *p<0.05

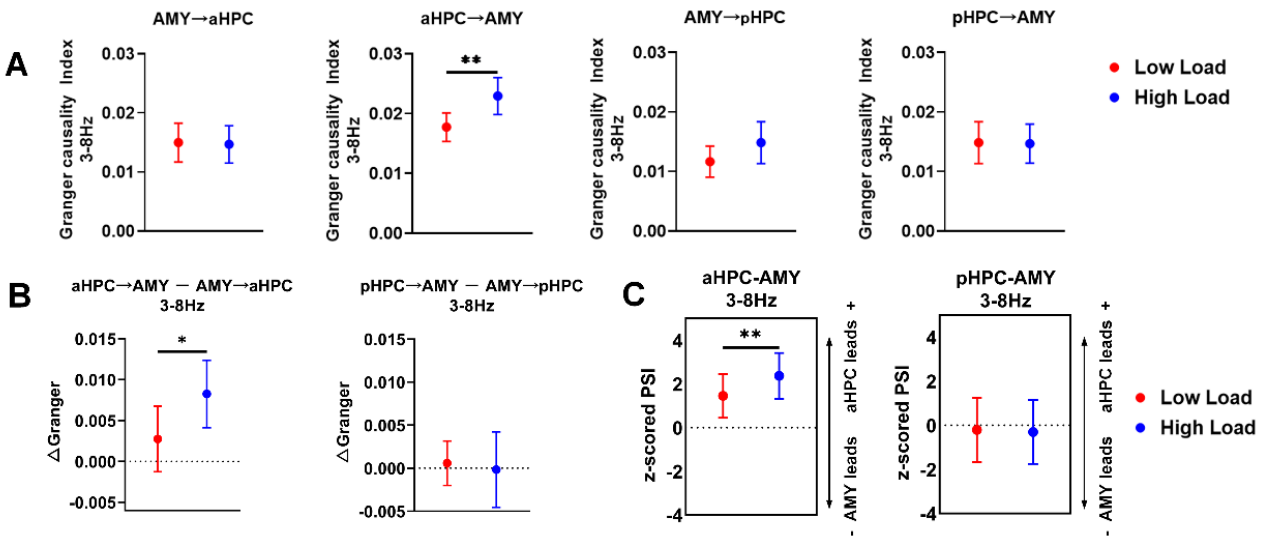

2.6. Load-dependent inter-regional phase-amplitude coupling between AMY and HPC during WM maintenance

Given that AMY theta-coupled HPC gamma activity tracked successful subsequent remember responses for emotional stimuli, we examined whether inter-regional PAC between AMY and HPC would be associated with successful WM maintenance.[61] PAC plays a crucial role in the flexible coordination of inter-regional information transfer, whereby the phase of slow oscillations dynamically adjusts the magnitude of high-frequency amplitude.[39] We performed inter-regional PAC analyses of both phase-amplitude combinations (low-frequency phase from AMY and high-frequency amplitude from aHPC or pHPC, and vice versa) for the correct trials. The averaged z-scored PAC showed that modulations of the theta phase of AMY entrained the gamma amplitude of aHPC/pHPC (AMY-aHPC: peak at 3 Hz and 33 Hz under both low- and high-load conditions; AMY-pHPC: peak at 4 Hz and 43 Hz under the low-load condition, 4 Hz and 93 Hz under the high-load condition) and the theta phase of aHPC/pHPC entrained the gamma amplitude of AMY (aHPC-AMY: peak at 6 Hz and 78 Hz under the low-load condition, 6 Hz and 88 Hz under the high-load condition; pHPC-AMY: peak at 7 Hz and 63 Hz under the low-load condition, 7 Hz and 53 Hz under the high-load condition) (**Figure 6A**).

We then evaluated whether the inter-regional PAC was task-induced or not. Our findings revealed that both AMY-aHPC/pHPC (AMY theta phase entraining aHPC/pHPC gamma amplitude) and aHPC/pHPC-AMY (aHPC/pHPC theta phase entraining AMY gamma amplitude) exhibited task-specific cross-frequency coupling for the correct trials under both the low- (AMY-aHPC: $p < 0.0001$; AMY-pHPC: $p = 0.0006$; aHPC-AMY: $p < 0.0001$; pHPC-AMY: $p = 0.0063$, Wilcoxon signed rank test) and the high-load conditions (AMY-aHPC: $p < 0.0001$; AMY-pHPC: $p = 0.0065$; aHPC-AMY: $p < 0.0001$; pHPC-AMY: $p < 0.0001$, Wilcoxon signed rank test) (**Figure 6B**). To further compare PAC between the two load conditions, we calculated the average theta-gamma PAC value and observed a significantly higher PAC under the high-load condition compared to the low-load condition for aHPC-AMY and pHPC-AMY ($p = 0.0027$, $p = 0.0004$, Wilcoxon signed rank test) (**Figure 6B**). These results suggest that inter-regional PAC between HPC and AMY supports the process of WM in a load-dependent manner, with the phase of HPC theta oscillations modulating the gamma amplitude of AMY during maintenance.

Figure 6. Inter-regional theta-gamma PAC between AMY and HPC for the correct trials. A) Averaged phase-amplitude comodulogram across electrode pairs during maintenance. Warmer colors denote higher z-scored PAC value. B) Extracted and averaged inter-regional theta-gamma PAC during baseline, low-load and high-load maintenance. 'AMY-aHPC' denotes AMY theta phase entraining aHPC gamma amplitude; while 'aHPC-AMY' indicates the reverse modulation. Error bars represent the SEM. ****$p<0.0001$, ***$p<0.001$, **$p<0.01$.

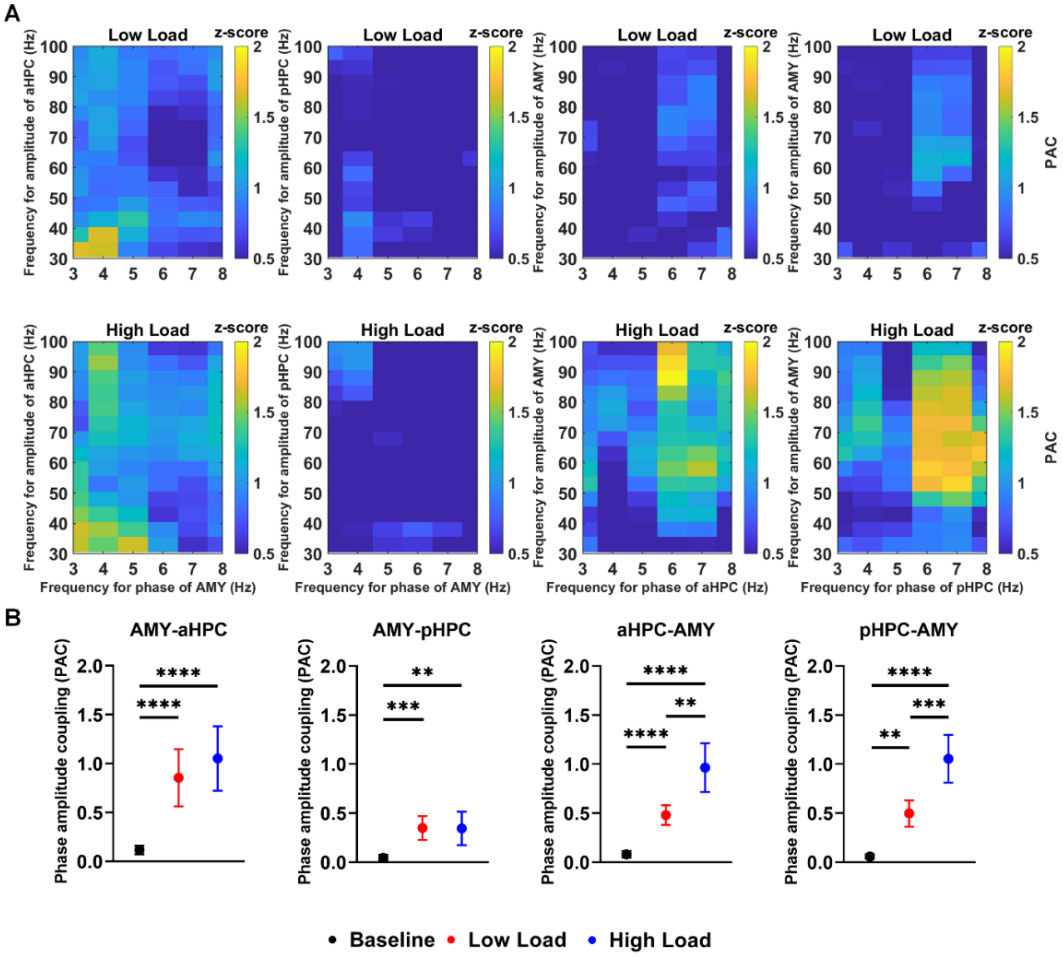

2.7. Absence of AMY-HPC interactions in the incorrect trials

Considering the maintenance process is involved in keeping novel information available and contributes significantly to successful behavioral performance, we investigated the specificity of the above findings to successful outcomes. We first analyzed the power change between baseline and maintenance for the incorrect trials. In the theta/alpha band, only AMY exhibited a significant task-induced increase in the theta/alpha power during maintenance ($p = 0.012$ and $p = 0.011$, one sample Wilcoxon test), whereas aHPC or pHPC showed no such change (theta band: $p = 0.9046$ and $p = 0.7609$; alpha band: $p = 0.1838$ and $p = 0.8034$, one sample Wilcoxon test) (**Figure 7A**). We then quantified intra-regional theta-gamma PAC during baseline and maintenance for the incorrect trials. This analysis revealed no significant task-induced PAC during maintenance in AMY ($P = 0.8028$, Wilcoxon signed rank test). In contrast, the PAC was greater during maintenance than baseline in aHPC and pHPC (aHPC: $p = 0.014$, pHPC: $p = 0.0073$, Wilcoxon signed rank test) (**Figure 7B**). These results show clear evidence that human AMY supports WM maintenance and exhibits different patterns with aHPC/pHPC.

Next, we assessed the theta band phase synchrony for AMY-aHPC and AMY-pHPC circuits for the incorrect trials, characteristics that showed task-relevance and load-dependency in preceding analyses. No significant difference between maintenance and baseline was found in the theta band ($p = 0.6291$ and $p = 0.9632$ for AMY-aHPC and AMY-pHPC, respectively, Wilcoxon signed rank test) (**Figure 7C**). Additionally, we analyzed the inter-regional theta-gamma PAC for the incorrect trials to explore whether cross-frequency AMY-HPC interactions during maintenance contributed to the behavioral success. Specifically, we compared the modulation of aHPC/pHPC theta phase entraining AMY gamma amplitude and AMY theta phase entraining aHPC/pHPC gamma amplitude between maintenance and baseline periods. The aHPC/pHPC-AMY PAC and AMY-pHPC PAC revealed no significant differences between maintenance and baseline period for the incorrect trials (aHPC-AMY: $p = 0.6058$, pHPC-AMY: $p = 0.0942$, AMY-pHPC: $p = 0.1018$, Wilcoxon signed rank test) (**Figure 7D)**. Although AMY-aHPC showed a significant increase during maintenance ($p = 0.0427$, Wilcoxon signed rank test), the PAC value of the incorrect trials (PAC value 0.2789) was obviously smaller than that of the correct trials (PAC value 0.9537). Together, these results indicate that task-induced theta synchrony and inter-regional theta-gamma PAC between AMY and HPC during maintenance facilitate successful WM behavior.

Figure 7. Intra-regional local activity and AMY-aHPC/pHPC interactions for the incorrect trials. A) Normalized theta (3–8 Hz) and alpha (8–13 Hz) power during maintenance in AMY, aHPC and pHPC. B) Intra-regional theta-gamma PAC in AMY, aHPC and pHPC during baseline and maintenance. C) AMY-aHPC/pHPC wPLI within the theta band during baseline and maintenance. D) Inter-regional theta-gamma PAC over AMY-aHPC/pHPC (AMY theta phase entraining aHPC/pHPC gamma amplitude) and aHPC/pHPC-AMY (aHPC/pHPC theta phase entraining AMY gamma amplitude) during baseline and maintenance. Error bars represent the SEM. $^{**}p<0.01$, $^{*}p < 0.05$.

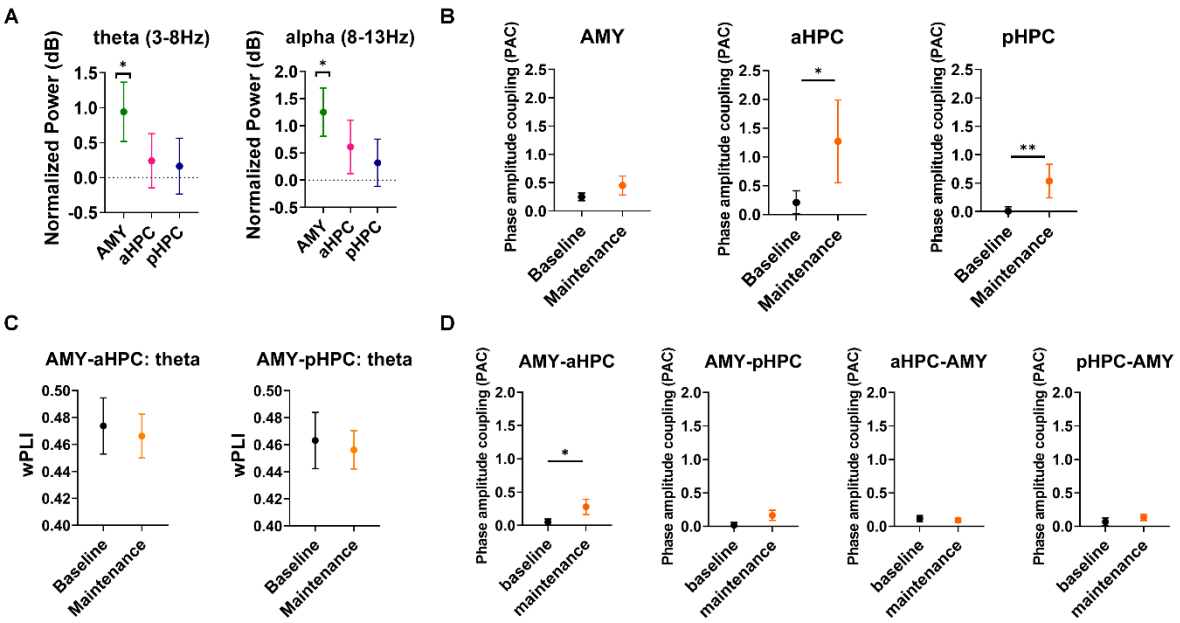

3. Discussion

In this study, we provide converging evidence that AMY play crucial roles in multi-item WM maintenance, with their specific oscillatory patterns and interaction strengths being load-dependent. Specifically, we found high load elicited increased low-frequency power and intra-regional theta-gamma PAC in AMY. On the circuit level, the modulation strength of HPC (including both aHPC and pHPC) theta phase entraining AMY gamma amplitude was enhanced under the high-load condition. Additionally, there was a noticeable increase in AMY-aHPC theta phase synchrony and directional connectivity strength under the high-load condition, directed from aHPC to AMY. In contrast, pHPC-AMY theta phase synchrony was not affected by memory load. Overall, our findings underscore the involvement of AMY in non-emotional WM task and emphasize the critical impact of AMY-HPC interactions in multi-item WM maintenance.

3.1. AMY activity support non-emotional WM maintenance

Our results demonstrated that theta and alpha power were elevated in both AMY and HPC during maintenance under the high-load condition. These findings regarding HPC align with previous studies that have indicated the involvement of human HPC in WM maintenance.[11,12] Theta rhythm has been proposed to be responsible for organizing WM items,[40] and alpha oscillations thought to protect WM maintenance against anticipated distractors have also been

associated with selective attention.[41,42] Importantly, in our study, similar load-dependent patterns in power were observed in AMY. Previous studies have demonstrated the presence of theta oscillations in AMY within the context of emotional arousal,[43,44] which could be a physiological substrate for the facilitated consolidation of emotional memories.[45] Our new findings extended these prior findings, revealing that theta oscillations in AMY are active even in non-emotional WM processes.

In addition to the load effect for the correct trials, we also preliminarily investigate the function of behavioral success. Our results indicate that increases in theta and alpha power in HPC during maintenance are associated with subsequent successful WM responses, which echoes the results of earlier research.[46] Interestingly, AMY still exhibited task-induced increased theta/alpha power during maintenance even when the items were not remembered. Previous studies have demonstrated that AMY is involved in the selective attention to goal-relevant stimuli without any emotional valence.[47,48] Our results suggest that AMY mediates the relevance appraisal function for the task-based needs.[49,50] In other words, task-relevant events requiring a subsequent response tend to elicit greater AMY activation, independent of behavioral performance.

Within human HPC, PAC has been recognized as a well-established mechanism for sequential memory organization and multi-item WM maintenance.[10,51,52] Our results showed that theta-gamma PAC in both aHPC and pHPC was significantly enhanced under the high-load condition. Previous fear-learning research has demonstrated an enhancement of PAC in AMY during periods of fear compared to the safety state.[53] However, it is unclear how AMY PAC mediates non-emotional WM under different load conditions. In this study, we found that the PAC in AMY was load-dependent in the correct trials, with enhanced coupling strength of gamma oscillations locking to the theta phase when multiple letters were required to be held during WM maintenance. Our findings suggest that the phase coding mode in AMY may not only assume a crucial function in emotional functions but also serve as a more general mechanism to support the flexible organization of complex mnemonic information.[54]

3.2. Load-dependent AMY-HPC interactions during WM maintenance

Phase synchrony is crucial to facilitating communication between different brain regions, contributing to cognitive flexibility in humans.[35] Theta synchrony of AMY-HPC has been

proposed to support fear memory consolidation and retrieval.[55–57] One study reported that the increased theta connectivity was correlated with WM load, which proved to be substantially involved in executive control.[58] This study found a load-dependent theta phase synchrony between AMY and HPC only in correctly performed trials, indicating that AMY-HPC circuits also contribute to non-emotional WM maintenance. These findings suggest that theta rhythm synchrony may serve as a general integrative mechanism of cognitive circuits with divergent connectivity patterns in response to varying cognitive demands.

Furthermore, our results showed that theta band information flow from aHPC to AMY was load-dependent during non-emotional WM maintenance. This corroborates prior studies, which highlighted the importance of information outflow from HPC in WM maintenance.[26,59] It has been suggested that HPC serves as a source of polymodal sensory information to AMY, which has been demonstrated to act as the relevance detector in relation to current goals and needs.[60,61] Some researchers considered the processes involved in WM maintenance to be primarily attentional processes.[62,63] Considering that high load may be related to high attentional control demands, it is plausible that the increased effective connectivity of AMY driven by aHPC may enhance attention to relevant stimuli and the formation of HPC-formed memories.[61]

Furthermore, enhanced WM load can lead to an increase in psychological stress that has a significant impact on the activity of AMY, primarily through the release of stress hormones. Previous human studies have shown that AMY-HPC interaction was associated with enhanced memory performance under stress.[64] Under stress conditions, the stress hormones induced by activation of the rapid autonomic nervous system, such as noradrenaline, could enhance memory not only by directly impacting on HPC but also by indirectly modulating HPC via AMY.[65,66] This modulation from AMY enhanced vigilance and increased HPC excitability, which may further improve WM maintenance under stress states.

The inter-regional PAC is thought to serve as a mechanism for organizing neural activity across different brain regions and has been proposed to modulate synaptic plasticity.[39,67] Numerous human emotional memory studies have reported PAC within AMY and HPC. For instance, the recognition of emotional stimuli and the formation of aversive memory were associated with AMY-HPC PAC between theta and gamma oscillations,[44,68] suggesting the information transformation via PAC between AMY and HPC to modulate multiple aspects of cognition. In this study, we observed that the coordination relationship of HPC theta phase entraining AMY

gamma amplitude was load-dependent during maintenance. Considering that gamma activity in human AMY is associated with task-related stimulus processing and memory consolidation,[69,70] the entrainment of AMY gamma oscillations to HPC theta phases may amplify the task-relevant neuronal representation and facilitate the behavioral consequences under the high-load condition.[71,72] This finding contrasts with the patterns observed in previous rodent and human studies, where the AMY theta phase was shown to regulate the activity of HPC, thereby facilitating memory consolidation and salient information processing.[19,73,74] On one hand, these previous results suggest the mechanism for long-term memory consolidation; however, they may not provide direct evidence of an effect on WM, especially under the high-load condition that requires remembering specific multiple information in a short period of time. On the other hand, the opposite modulation pattern of PAC during the processing of emotionally salient events may reflect that emotional contents and WM load have opposite effects on attention.[75] Overall, our findings provide direct evidence that the inter-regional cross-frequency coupling in HPC-AMY contributes to non-emotional WM maintenance in a load-dependent manner, with stronger coupling of HPC theta phase entraining AMY gamma amplitude observed under the high load condition.

3.3. AMY-HPC interactions contribute to behavioral success

The synchrony at theta frequencies between AMY and HPC during encoding is thought to play a critical role in successful immediate memorization of repeated words, and this theta synchrony would enhance information transfer and processing between AMY and HPC.[76] We found that the task-induced theta synchrony during maintenance was associated with behavioral success, implicating synchronous theta oscillations may be a general mechanism mediating human memory. Although most studies examining AMY-HPC interactions focused on how AMY influences HPC-dependent memories,[19,25,73] it is important to emphasize here that HPC-to-AMY pathways are equally critical because our results demonstrated that the bidirectional interaction between AMY and HPC (including both aHPC and pHPC) is crucial for behavioral success in non-emotional WM. A possible explanation could be that the information highly processed in HPC could be then sent to AMY, which in turn modulates neural activity in several target areas to guide attention and exert a modulatory influence on HPC-dependent memory systems.[77,78] One popular view is that selective attention is one of the potential mechanisms for maintenance and influences WM performance.[79-81] AMY is necessary for selective attention; it is a central perceptual node where multimodal information converges, and the

output of AMY will guide perception and covert attention, and overt reorienting.[82] In this regard, we assume that AMY is driven to facilitate attention to task-relevant information during maintenance and AMY-HPC interaction plays an important role in incorporating WM items into neural representations.

Human studies have demonstrated that AMY-HPC communication via cross-frequency coupling can support emotional memory encoding and successful pattern separation of emotional information, in which the AMY theta phase to HPC broadband gamma activity couples was found to determine subsequent remembering of emotional stimuli, and the HPC-AMY theta-gamma PAC decreases during incorrect memory recognition with emotional stimulus.[44,68] We provide evidence that interregional communication between AMY and HPC via theta-gamma phase-amplitude coupling supports successful non-emotional WM maintenance. These results support the view that inter-regional PAC is a crucial neurophysiological mechanism underlying memory processing.[83] Taken together, these findings underscore the importance of AMY-HPC interactions during WM maintenance for successful task performance.

3.4. Divergent connectivity patterns of AMY to aHPC and pHPC

The interconnections between AMY and distinct HPC regions are robust and complex. Here, our results indicate that theta phase synchrony between AMY and HPC subregions exhibits distinct connectivity patterns during maintenance. Specifically, we found that aHPC-AMY interactions in the theta band showed load dependency, whereas the connectivity between pHPC and AMY was not affected by load. In particular, the information flow from aHPC to AMY in the theta band was observed to increase under the high-load condition. These results reveal HPC subregions exhibit different connectivity with AMY.[84,85]

One possible explanation for the observed functional difference is that the transmembrane currents giving rise to AMY theta oscillations are likely generated by synaptic inputs from HPC, mostly glutamatergic.[86] Classical horseradish peroxidase studies suggest that there are differences in the efferent fibers of HPC between its subregions, with ventral HPC preferentially projecting to AMY.[28,87] This is also supported by previous rodent studies, which indicated that the dorsal and ventral portions of HPC are distinct functionally.[88,89] Considering the essential role of HPC in the attention process,[90,91] particularly the key role of the afferent projections

from ventral HPC in the cognitive process of selective attention in rodents,[92] a plausible explanation for aHPC-to-AMY information flow might be its involvement in the control of selective attention under the high-load condition.

While observing the load-dependent theta phase synchrony between aHPC and AMY, we also found significant and intense modulation of inter-regional theta-gamma PAC for both aHPC-AMY and pHPC-AMY under the high-load condition. The wPLI is a metric used to quantify the coupling between oscillations of the same frequency, whereas PAC estimates how the neural populations interact across frequency bands.[93,94] However, there is still no consensus on whether these two phenomena are directly related to each other. One previous study suggests that both same-frequency coupling and cross-frequency coupling may be part of the same mechanism for inter-regional communication.[94] Contrarily, other studies have reported no strong overlap between phase synchrony and inter-regional PAC.[95] Our results suggest that the inter-regional PAC may not be directly explained by theta phase synchrony, supporting the opinion that it is necessary to evaluate multiple coupling measures to quantify the inter-regional correlation.[96]

4. Conclusion

The present research aimed to explore the role of AMY and AMY-HPC circuit in multi-item WM maintenance. Although human AMY and its interaction with HPC have primarily been associated with supporting emotion associated-memory and long-term memory, the role of AMY and its interaction with HPC in supporting non-emotional WM and the underlying neural mechanisms have remained largely unexplored. To address these quentions, we quantified the effect of memory load on intra-regional neural characteristics and inter-regional connectivity metrics during WM maintenance. Our findings revealed enhanced low-frequency power and intra-regional PAC under the high-load condition in both AMY and HPC (including both aHPC and pHPC). On the network level, a high WM load elicited an increase in the inter-regional PAC of HPC theta phase entraining AMY gamma amplitude. Furthermore, our analysis revealed different connectivity patterns between AMY and HPC subregions, where AMY-aHPC exhibited load-dependent theta phase synchrony and an effective connectivity from aHPC to AMY, whereas the connectivity between AMY and pHPC in the theta band remained unchanged across different load conditions. In conclusion, our study offers evidence supporting the functional involvement of AMY in non-emotional

higher-level cognitive processes and provides a novel insight into the neurophysiological basis of human AMY and AMY-HPC interactions during WM maintenance.

5. Experimental Section

Subjects and electrodes: We analyzed an iEEG dataset from nine right-handed patients, all of whom were diagnosed with drug-resistant focal epilepsy.[31] These patients had intracranial depth electrodes (1.3 mm diameter, 8 contacts of 1.6 mm length, spacing between contact centers 5 mm, ADTech®, Racine, WI, www.adtechmedical.com) implanted stereotactically for the potential surgical treatment of epilepsy. The configurations for electrode implantation were determined solely based on clinical needs. Each subject gave informed consent before the experiment. This study was approved by the institutional ethics review board (Kantonale Ethikkommission Zürich, PB-2016-02055).

Data acquisition and electrode localization: The iEEG recordings were done against a common intracranial reference via the Neuralynx ATLAS recording system (0.5-5000Hz passband, Neuralynx®, Bozeman, MT, USA). The sampling rate of iEEG recordings was 2000Hz. Electrodes were localized in each subject using post-implantation CT scans and post-implantation structural T1-weighted MRI scans. The dataset offered the normalized MNI coordinates of each contact and corresponding anatomical label assigned by Brainnetome Atlas.[97]

Experimental design: Subjects performed a modified Sternberg task, which incorporated temporally separated epochs of encoding, maintenance and retrieval period of WM (**Figure 1A)**. Each trial started with a blank screen with fixation square for 1 second (fixation period), followed by the presentation of a set of 4, 6, or 8 letters in the center of the screen surrounded by 'X'. The letter 'X' was not part of the set to be memorized. WM load was determined by the number of letters. The stimulus was presented for 2 second (encoding period). Following the encoding period, the stimulus disappeared from the screen and replaced by a fixation square for 3 seconds (maintenance period). After the maintenance period, a probe letter appeared. Subject were instructed to respond rapidly to indicated whether the probe letter was part of the stimulus set by pressing a button ("IN" or "OUT"). A session consisted of 50 trials, lasting approximately 10 minutes. Each subject completed 2−7 sessions in the dataset.

Channel selection and pre-processing: Due to clinical consideration, the targeted regions and hemispheres varied among subjects (**Table 1**). To minimize inter-individual variability, the two most medial channels were selected on each electrode targeting AMY and aHPC and pHPC in each hemisphere, in accordance with previous studies.[98,99] In total, we identified 32 aHPC, 32 pHPC and 30 AMY contacts across all subjects (the locations in the standard MNI space are shown in **Figure 1C**). For the inter-regional analysis, only ipsilateral channel pairs were included.

Data preprocessing was performed using the EEGLAB,[100] FieldTrip (http://fieldtrip.fcdonders.nl/) toolboxes and custom MATLAB (Mathworks, Natick MA, USA) scripts. First, we performed bipolar reference by subtracting the signal from the contact closest to the channel of interest. Bipolar re-referencing has been suggested to effectively improve sensitivity and reduce artifacts by eliminating distant signals picked up by adjacent electrode contacts.[101] After bipolar re-referencing, the iEEG recordings were band-pass filtered between 1−200 Hz using the fourth-order Butterworth filter with Hamming window. Only trials with correct behavioral responses were included in our analysis of load effect. Then we concatenated these trials and Z-transformed the signals of each channel separately by removing mean and scaling by the standard deviation. We epoched the continuous data into trials, and then rejected any trials had been visually inspected as containing artifacts (with 82.6% of all correct epochs remaining in the analysis).

Table 1. Number of intracranial contacts for AMY, aHPC and pHPC.

Subject	AMY (left)	AMY (right)	aHPC (left)	aHPC (right)	pHPC (left)	pHPC (right)
1	8	0	8	0	8	8
2	8	8	8	8	8	8
3	8	0	8	8	8	0
4	8	8	8	8	8	8
5	8	0	8	0	0	8
6	8	8	8	8	8	8
7	8	8	8	8	8	8
8	8	8	8	8	8	7
9	8	8	8	8	8	8

Spectral power analysis: Time-frequency representations of power were computed for low-load (set size 4) and high-load (set size 6) trials in AMY, aHPC and pHPC. We used the wavelet method (with number of cycles 6) implemented in Fieldtrip. We computed power in 1 Hz steps across frequency ranging from 3 Hz to 100 Hz with a time resolution of 0.01 s. The power from 0.5 to 0 s before stimulus onset served as a baseline power. We corrected the baseline by transforming the power estimates to decibels relative to the baseline power. When comparing the normalized power at each time-frequency point between different load conditions, we used cluster-based nonparametric permutation tests (with 2000 permutations). Then, theta and alpha power were calculated by averaging the normalized power over 3–8 Hz and 8–13 Hz, respectively. A paired Wilcoxon signed rank test was used to compare the low-frequency power between the two load conditions.

Inter-regional phase synchrony: To evaluate the functional connectivity between AMY and aHPC/pHPC, we calculated the wPLI, which is less sensitive to the volume conduction driven by a single or common source.[37] The wPLI is solely based on the imaginary part of the cross-spectrum between two signals and has been shown to exhibit the best performance in the presence of noise compared to other phase statistics.[102] The wPLI was computed as follows:

$$\mathrm{wPLI} = \frac{\left|\sum_{n=1}^{N} \Im\{X_n\}\right|}{\sum_{n=1}^{N} \left|\Im\{X_n\}\right|} \qquad (1)$$

where N is the total number of trials, $\Im\{X_n\}$ represents the imaginary part of the cross-spectrum in the nth trial. We used the same time-frequency decomposition parameters as used for the spectral power analysis to obtain phase information. The wPLI ranges from 0 to 1, with values approaching 1 indicating stronger phase synchrony.

To avoid any bias due to the different number of trials for the two load conditions, the trials number was matched to the lower number of the two conditions by random selection. Before calculating the wPLI for each electrode pair and condition, the trial-wise mean was subtracted from each trial to minimize contamination from simultaneous voltage changes on phase estimations.[103] To test the statistical significance of the wPLI, we shuffled trials of all conditions 200 times to create a null distribution and computed the 95th percentile threshold. We averaged the null distribution of all electrode pairs and compared the observed wPLI with this null distribution. Only the electrode pairs with wPLI values above the corresponding threshold were selected for further analysis. Next, we extracted and averaged the wPLI within

the theta (3–8 Hz) and alpha (8–13 Hz) bands and compared the wPLI estimates for the low- and high-load conditions within each band by use of paired Wilcoxon signed rank test.

Granger causality analysis: To examine the directionality of the AMY-aHPC and AMY-pHPC synchrony, we analyzed the effective connectivity in the theta band within the maintenance period. We applied the Multivariate Granger Causality (MVGC) Toolbox (based on the Akaike information criterion to define the model order) computing the spectral GC within the theta band (3–8 Hz) for the electrode pairs that showed significant theta phase synchrony.[104] The GC index was computed for the low- and high-load trials, separately. The significance testing was conducted by creating the null distribution of GC, which was created by randomly shuffling and switching directions across trials for each electrode pairs 200 times. The GC estimates were considered significant if they exceeded the threshold of 95th percentile of the null distribution. We extracted the GC index from significant electrode pairs for both directions within each circuit (AMY-aHPC: AMY to aHPC, aHPC to AMY; AMY-pHPC: AMY to pHPC, pHPC to AMY). To estimate the effect of load on the effective connectivity strength, we used Wilcoxon signed rank test to compare the GC index between low- and high-load trials for each direction of each circuit.

Within-frequency phase-slope index: In order to reduce spurious connectivity arising from volume conduction effects and provide a more robust measurement, we re-assessed the inter-regional directionality in the theta band using the PSI from both directions for aHPC-AMY and pHPC-AMY circuits.[38] First, the trial-wise mean was subtracted from each trial of the low- and high-load conditions. Then the PSI was computed for each electrode pair from different brain regions in the frequency band of 3–8 Hz during WM maintenance period as described by Nolte et al..[38] The PSI estimates the slope of the phase difference between the sender signals and receiver signals, which positive PSI indicates that the seed region acts as a sender (modulating signals), and negative values indicates the seed region acts as a receiver (modulated signals). To assess the significance level of PSI, we randomly shuffled the trials 200 times to generate null distribution for each electrode pair. The raw PSI were z-scored on the null distribution. Significant PSI was defined as $|z| > 1.96$ (i.e., $\alpha = 0.05$). Then we extracted the electrode pairs with significant z-scored PSI for further analysis. To confirm whether the directional information flow was modulated by WM load, we comparsed the PSI values between the low- and high-load conditions using Wilcoxon signed rank test.

Intra- and inter-regional cross frequency phase amplitude coupling analysis: The cross-frequency PAC was estimated within and between regions using Tort's method of modulation index (MI).[105] We estimated the phase of low frequencies between 2 and 20 Hz (in steps of 1 Hz; termed "low-frequency phase") and amplitude of frequencies between 30 and 100 Hz (in steps of 5 Hz; termed "high-frequency amplitude") and computed the MI under both conditions. In brief, we first obtained the instantaneous power and phase representations using the Morlet convolution with a width of seven cycles for each epoch. Then the maintenance intervals were extracted and concatenated back into one continual EEG signal for each channel. The low-frequency phases were divided in 20 bins (i.e., 18° per phase bin), and the mean amplitude of high-frequency oscillations was calculated in each bin. The distribution across bins was uniform if the PAC is not evident. A normalized version of the Kullback-Leibler divergence was used to measure the distribution of this histogram and create MI values. This procedure was repeated for all phase-amplitude frequency pairs. For inter-regional PAC, we performed two directions estimates: the theta phase of AMY modulating the gamma amplitude of aHPC/pHPC and the theta phase of aHPC/pHPC modulating the gamma amplitude of AMY for the low- and high-load conditions.

To test the significance of the raw PAC, we used surrogate test as was done in previous studies. Specifically, we randomly generated the time lag of the raw phase time series the temporal relationship between phase and amplitude information, and recompute the PAC using the shuffled phase time series. This procedure was repeated 200 times to create the null distribution of PAC values. The raw PAC values were then z-scored against the null distributions to correct for any spurious results and evaluate the significance of the PAC values. Z-scored PAC values that exceed a threshold value of 1.96 were considered significant.[95] Only single channels from target regions (for intra-regional PAC estimate) or electrode pairs from two regions within the same hemisphere (for intra-regional PAC estimate) exhibiting significant PAC values were included in subsequent analyses. We then averaged the theta (3–8 Hz)-gamma (30–100 Hz) z-scored PAC values for the low- and high-load trials, respectively. A Wilcoxon signed rank test was applied to estimate the effect of load on intra-regional PAC and inter-regional PAC.

References

[1] A. D. Baddeley, G. Hitch, in *Psychology of Learning and Motivation*, Elsevier, **1974**, pp. 47–89.

[2] E. L. Johnson, J. W. Y. Kam, A. Tzovara, R. T. Knight, *J. Neural Eng.* **2020**, *17*, 051001.

[3] C. F. Geier, K. Garver, R. Terwilliger, B. Luna, *Journal of Neurophysiology* **2009**, *101*, 84.

[4] Y. G. Pavlov, B. Kotchoubey, *Psychophysiology* **2020**, DOI 10.1111/psyp.13735.

[5] M. Leszczyński, J. Fell, N. Axmacher, *Cell Reports* **2015**, *13*, 1272.

[6] L. Brockhoff, S. Schindler, M. Bruchmann, T. Straube, *Neuroscience & Biobehavioral Reviews* **2022**, *135*, 104580.

[7] A. Schaefer, T. S. Braver, J. R. Reynolds, G. C. Burgess, T. Yarkoni, J. R. Gray, *Journal of Neuroscience* **2006**, *26*, 10120.

[8] K. Schon, Y. T. Quiroz, M. E. Hasselmo, C. E. Stern, *Cerebral Cortex* **2009**, *19*, 2561.

[9] K. Schon, R. E. Newmark, R. S. Ross, C. E. Stern, *Cereb. Cortex* **2016**, *26*, 1965.

[10] N. Axmacher, M. M. Henseler, O. Jensen, I. Weinreich, C. E. Elger, J. Fell, *Proc. Natl. Acad. Sci. U.S.A.* **2010**, *107*, 3228.

[11] E. Boran, T. Fedele, P. Klaver, P. Hilfiker, L. Stieglitz, T. Grunwald, J. Sarnthein, *Sci. Adv.* **2019**, *5*, eaav3687.

[12] A. Brzezicka, J. Kamiński, C. M. Reed, J. M. Chung, A. N. Mamelak, U. Rutishauser, *Journal of Cognitive Neuroscience* **2019**, *31*, 1290.

[13] H. Ye, G. Li, X. Sheng, X. Zhu, *J. Neural Eng.* **2022**, *19*, 026043.

[14] J. Kamiński, S. Sullivan, J. M. Chung, I. B. Ross, A. N. Mamelak, U. Rutishauser, *Nat Neurosci* **2017**, *20*, 590.

[15] L. D. Voogd, E. J. Hermans, *Human Brain Mapping* **2022**, *43*, 2951.

[16] J. L. McGaugh, L. Cahill, B. Roozendaal, *Proc. Natl. Acad. Sci. U.S.A.* **1996**, *93*, 13508.

[17] B. Roozendaal, N. A. Castello, G. Vedana, A. Barsegyan, J. L. McGaugh, *Neurobiology of Learning and Memory* **2008**, *90*, 576.

[18] A. Barsegyan, J. L. McGaugh, B. Roozendaal, *Frontiers in Behavioral Neuroscience* **2014**, *8*.

[19] C. S. Inman, J. R. Manns, K. R. Bijanki, D. I. Bass, S. Hamann, D. L. Drane, R. E. Fasano, C. K. Kovach, R. E. Gross, J. T. Willie, *Proc. Natl. Acad. Sci. U.S.A.* **2018**, *115*, 98.

[20] J. Kamiński, A. Brzezicka, A. N. Mamelak, U. Rutishauser, *Neuron* **2020**, *106*, 256.

[21] E. Boran, P. Hilfiker, L. Stieglitz, J. Sarnthein, P. Klaver, *NeuroImage* **2022**, *254*, 119123.

[22] T. B. Christophel, P. C. Klink, B. Spitzer, P. R. Roelfsema, J.-D. Haynes, *Trends in Cognitive Sciences* **2017**, *21*, 111.

[23] G. Richter-Levin, I. Akirav, *MN* **2000**, *22*, 011.

[24] R. Roesler, M. B. Parent, R. T. LaLumiere, C. K. McIntyre, *Neurobiology of Learning and Memory* **2021**, *184*, 107490.

[25] E. A. Phelps, *Current Opinion in Neurobiology* **2004**, *14*, 198.

[26] J. Li, D. Cao, S. Yu, X. Xiao, L. Imbach, L. Stieglitz, J. Sarnthein, T. Jiang, *Nat Commun* **2023**, *14*, 2921.

[27] A. J. McDonald, D. D. Mott, *Journal of Neuroscience Research* **2017**, *95*, 797.

[28] B. A. Strange, M. P. Witter, E. S. Lein, E. I. Moser, *Nat Rev Neurosci* **2014**, *15*, 655.

[29] L. C. Dandolo, L. Schwabe, *Nat Commun* **2018**, *9*, 1205.

[30] H. Zhu, K. E. Pleil, D. J. Urban, S. S. Moy, T. L. Kash, B. L. Roth, *Neuropsychopharmacol* **2014**, *39*, 1880.

[31] E. Boran, T. Fedele, A. Steiner, P. Hilfiker, L. Stieglitz, T. Grunwald, J. Sarnthein, *Sci Data* **2020**, *7*, 30.

[32] D. A. Pinotsis, T. J. Buschman, E. K. Miller, *Cerebral Cortex* **2019**, *29*, 1670.

[33] J. Lisman, *Hippocampus* **2005**, *15*, 913.

[34] A. Bahramisharif, O. Jensen, J. Jacobs, J. Lisman, *PLoS Biol* **2018**, *16*, e2003805.

[35] P. Fries, *Trends in Cognitive Sciences* **2005**, *9*, 474.

[36] C. Schmiedt, A. Brand, H. Hildebrandt, C. Basar-Eroglu, *Cognitive Brain Research* **2005**, *25*, 936.

[37] M. Vinck, R. Oostenveld, M. van Wingerden, F. Battaglia, C. M. A. Pennartz, *NeuroImage* **2011**, *55*, 1548.

[38] G. Nolte, A. Ziehe, V. V. Nikulin, A. Schlögl, N. Krämer, T. Brismar, K.-R. Müller, *Phys. Rev. Lett.* **2008**, *100*, 234101.

[39] J. Fell, N. Axmacher, *Nat Rev Neurosci* **2011**, *12*, 105.

[40] F. Roux, P. J. Uhlhaas, *Trends in Cognitive Sciences* **2014**, *18*, 16.

[41] M. Bonnefond, O. Jensen, *Current Biology* **2012**, *22*, 1969.

[42] L.-M. Schönfeld, L. Wojtecki, *Front. Neurosci.* **2019**, *13*, 366.

[43] A. H. Taub, R. Perets, E. Kahana, R. Paz, *Neuron* **2018**, *97*, 291.

[44] J. Zheng, R. F. Stevenson, B. A. Mander, L. Mnatsakanyan, F. P. K. Hsu, S. Vadera, R. T. Knight, M. A. Yassa, J. J. Lin, *Neuron* **2019**, *102*, 887.

[45] D. Paré, *Trends in Cognitive Sciences* **2002**, *6*, 306.

[46] J. Li, D. Cao, V. Dimakopoulos, W. Shi, S. Yu, L. Fan, L. Stieglitz, L. Imbach, J. Sarnthein, T. Jiang, *J. Neurosci.* **2022**, *42*, 443.

[47] K. R. Laurens, K. A. Kiehl, P. F. Liddle, *Human Brain Mapping* **2005**, *24*, 35.

[48] K. A. Kiehl, M. C. Stevens, K. R. Laurens, G. Pearlson, V. D. Calhoun, P. F. Liddle, *NeuroImage* **2005**, *25*, 899.

[49] R. Guex, C. Méndez-Bértolo, S. Moratti, B. A. Strange, L. Spinelli, R. J. Murray, D. Sander, M. Seeck, P. Vuilleumier, J. Domínguez-Borràs, *Sci Rep* **2020**, *10*, 11138.

[50] O. T. OUSDAL, J. JENSEN, A. SERVER, A. R. HARIRI, P. H. NAKSTAD, O. A. ANDREASSEN, *Neuroscience* **2008**, *156*, 450.

[51] J. E. Lisman, O. Jensen, Neuron 2013, 77, 1002.

[52] J. Daume, J. Kamiński, A. G. P. Schjetnan, Y. Salimpour, U. Khan, M. Kyzar, C. M. Reed, W. S. Anderson, T. A. Valiante, A. N. Mamelak, U. Rutishauser, *Nature* **2024**, *629*, 393.

[53] J. M. Stujenske, E. Likhtik, M. A. Topiwala, J. A. Gordon, Neuron 2014, 83, 919.

[54] A. C. Heusser, D. Poeppel, Y. Ezzyat, L. Davachi, *Nat Neurosci* **2016**, *19*, 1374.

[55] R. T. Narayanan, T. Seidenbecher, C. Kluge, J. Bergado, O. Stork, H.-C. Pape, *European Journal of Neuroscience* **2007**, *25*, 1823.

[56] J. Lesting, R. T. Narayanan, C. Kluge, S. Sangha, T. Seidenbecher, H.-C. Pape, *PLoS ONE* **2011**, *6*, e21714.

[57] D. Popa, S. Duvarci, A. T. Popescu, C. Léna, D. Paré, *Proc. Natl. Acad. Sci. U.S.A.* **2010**, *107*, 6516.

[58] B. Griesmayr, B. Berger, R. Stelzig-Schoeler, W. Aichhorn, J. Bergmann, P. Sauseng, *Cogn Affect Behav Neurosci* **2014**, *14*, 1340.

[59] V. Dimakopoulos, P. Mégevand, L. H. Stieglitz, L. Imbach, J. Sarnthein, *eLife* **2022**, *11*, e78677.

[60] P. Sah, E. S. L. Faber, M. Lopez De Armentia, J. Power, *Physiological Reviews* **2003**, *83*, 803.

[61] J. LeDoux, *Neuron* **2012**, *73*, 653.

[62] N. Cowan, *Attention and Memory: An Integrated Framework*, Oxford University Press, New York, NY, US, **1995**.

[63] A. Kiyonaga, T. Egner, *Psychon Bull Rev* **2013**, *20*, 228.

[64] L. D. de Voogd, F. Klumpers, G. Fernández, E. J. Hermans, *Psychoneuroendocrinology* **2017**, *75*, 192.

[65] M. Joëls, T. Z. Baram, *Nat Rev Neurosci* **2009**, *10*, 459.

[66] E. V. Goldfarb, *Brain Cogn* **2019**, *133*, 94.
[67] R. T. Canolty, R. T. Knight, *Trends in Cognitive Sciences* **2010**, *14*, 506.
[68] M. Costa, D. Lozano-Soldevilla, A. Gil-Nagel, R. Toledano, C. R. Oehrn, L. Kunz, M. Yebra, C. Mendez-Bertolo, L. Stieglitz, J. Sarnthein, N. Axmacher, S. Moratti, B. A. Strange, *Nat Commun* **2022**, *13*, 6403.
[69] K. Müsch, C. M. Hamamé, M. Perrone-Bertolotti, L. Minotti, P. Kahane, A. K. Engel, J.-P. Lachaux, T. R. Schneider, *Cortex* **2014**, *60*, 34.
[70] V. Kanta, D. Pare, D. B. Headley, *Nat Commun* **2019**, *10*, 3970.
[71] P. Lakatos, G. Karmos, A. D. Mehta, I. Ulbert, C. E. Schroeder, *Science* **2008**, *320*, 110.
[72] C. E. Schroeder, P. Lakatos, *Trends in Neurosciences* **2009**, *32*, 9.
[73] N. S. Ahlgrim, J. R. Manns, *Front. Behav. Neurosci.* **2019**, *13*, 87.
[74] J. Zheng, K. L. Anderson, S. L. Leal, A. Shestyuk, G. Gulsen, L. Mnatsakanyan, S. Vadera, F. P. K. Hsu, M. A. Yassa, R. T. Knight, J. J. Lin, *Nat Commun* **2017**, *8*, 14413.
[75] A. MacNamara, J. Ferri, G. Hajcak, *Cogn Affect Behav Neurosci* **2011**, *11*, 321.
[76] C. Babiloni, F. Vecchio, G. Mirabella, M. Buttiglione, F. Sebastiano, A. Picardi, G. Di Gennaro, P. P. Quarato, L. G. Grammaldo, P. Buffo, V. Esposito, M. Manfredi, G. Cantore, F. Eusebi, *Human Brain Mapping* **2009**, *30*, 2077.
[77] M. Davis, P. J. Whalen, *Mol Psychiatry* **2001**, *6*, 13.
[78] M. G. Packard, L. A. Teather, *Neurobiology of Learning and Memory* **1998**, *69*, 163.
[79] A. Gazzaley, A. C. Nobre, *Trends in Cognitive Sciences* **2012**, *16*, 129.
[80] B. R. Postle, *Neuroscience* **2006**, *139*, 23.
[81] E. Awh, J. Jonides, *Trends in Cognitive Sciences* **2001**, *5*, 119.
[82] R. H. A. H. Jacobs, R. Renken, A. Aleman, F. W. Cornelissen, *Neuroscience & Biobehavioral Reviews* **2012**, *36*, 2069.
[83] J. Li, D. Cao, S. Yu, H. Wang, L. Imbach, L. Stieglitz, J. Sarnthein, T. Jiang, *J. Neurosci.* **2024**, *44*, e0398232023.
[84] N. V. Gulyaeva, *Neurochem Res* **2019**, *44*, 1306.
[85] G. Grigoryan, M. Segal, *Neural Plasticity* **2016**, *2016*, 1.
[86] M. Bocchio, S. Nabavi, M. Capogna, *Neuron* **2017**, *94*, 731.
[87] A. Pitkänen, M. Pikkarainen, N. Nurminen, A. Ylinen, *Annals of the New York Academy of Sciences* **2006**, *911*, 369.
[88] D. M. Bannerman, J. N. P. Rawlins, S. B. McHugh, R. M. J. Deacon, B. K. Yee, T. Bast, W.-N. Zhang, H. H. J. Pothuizen, J. Feldon, *Neurosci Biobehav Rev* **2004**, *28*, 273.
[89] A. B. Satpute, J. A. Mumford, B. D. Naliboff, R. A. Poldrack, *Emotion* **2012**, *12*, 58.

[90] K. M. O'Craven, P. E. Downing, N. Kanwisher, *Nature* **1999**, *401*, 584.

[91] Z.-X. Liu, K. Shen, R. K. Olsen, J. D. Ryan, *J. Neurosci.* **2017**, *37*, 599.

[92] X. Li, W. Chen, K. Pan, H. Li, P. Pang, Y. Guo, S. Shu, Y. Cai, L. Pei, D. Liu, H. K. Afewerky, Q. Tian, L.-Q. Zhu, Y. Lu, *Nat Neurosci* **2018**, *21*, 1239.

[93] A. Hyafil, A.-L. Giraud, L. Fontolan, B. Gutkin, *Trends in Neurosciences* **2015**, *38*, 725.

[94] J. González, M. Cavelli, A. Mondino, N. Rubido, A. BL Tort, P. Torterolo, *Neuroscience* **2020**, *449*, 157.

[95] D. X. Wang, K. Schmitt, S. Seger, C. E. Davila, B. C. Lega, *Hippocampus* **2021**, *31*, 481.

[96] D. Strahnen, S. K. T. Kapanaiah, A. M. Bygrave, D. Kätzel, *BMC Biol* **2021**, *19*, 24.

[97] L. Fan, H. Li, J. Zhuo, Y. Zhang, J. Wang, L. Chen, Z. Yang, C. Chu, S. Xie, A. R. Laird, P. T. Fox, S. B. Eickhoff, C. Yu, T. Jiang, *Cereb. Cortex* **2016**, *26*, 3508.

[98] C. R. Oehrn, S. Hanslmayr, J. Fell, L. Deuker, N. A. Kremers, A. T. Do Lam, C. E. Elger, N. Axmacher, *Journal of Neuroscience* **2014**, *34*, 10438.

[99] D. Pacheco Estefan, M. Sánchez-Fibla, A. Duff, A. Principe, R. Rocamora, H. Zhang, N. Axmacher, P. F. M. J. Verschure, *Nat Commun* **2019**, *10*, 2255.

[100] A. Delorme, S. Makeig, *Journal of Neuroscience Methods* **2004**, *134*, 9.

[101] G. Arnulfo, J. Hirvonen, L. Nobili, S. Palva, J. M. Palva, *NeuroImage* **2015**, *112*, 114.

[102] E. Wianda, B. Ross, *Brain Behav* **2019**, *9*, e01263.

[103] E. L. Johnson, J. N. Adams, A.-K. Solbakk, T. Endestad, P. G. Larsson, J. Ivanovic, T. R. Meling, J. J. Lin, R. T. Knight, *PLoS Biol* **2018**, *16*, e2004274.

[104] L. Barnett, A. K. Seth, *Journal of Neuroscience Methods* **2014**, *223*, 50.

[105] A. B. L. Tort, R. Komorowski, H. Eichenbaum, N. Kopell, *Journal of Neurophysiology* **2010**, *104*, 1195.